Available online at www.sciencedirect.com

SCIENCE DIRECT®

Proceedings of the Combustion Institute 30 (2005) 2345–2352

Proceedings of the Combustion Institute

www.elsevier.com/locate/proci

Inhibition of premixed and nonpremixed flames with phosphorus-containing compounds

A.G. Shmakov[a], O.P. Korobeinichev[a,*], V.M. Shvartsberg[a], D.A. Knyazkov[a], T.A. Bolshova[a], I.V. Rybitskaya[b]

[a] *Institute of Chemical Kinetics and Combustion, Novosibirsk 630090, Russia*
[b] *Novosibirsk State University, Novosibirsk 630090, Russia*

Abstract

The inhibition/extinction of various flames—premixed stoichiometric C_3H_8/air, nonpremixed counterflow $CH_4/O_2/N_2$, and nonpremixed coflow *n*-heptane/air cup-burner flames doped with a number of phosphorus-containing compounds (PCCs)—has been investigated experimentally. More than 20 PCCs (organic phosphates, phosphonates, phosphates) and their fluorinated derivatives were studied. All PCCs exhibited similar dependencies in burning velocities, extinction strain rates, and extinction volume fractions of CO_2 upon PCC loading in the range of mole fractions of 0–7000 ppm within an experimental deviation of ±5%. This confirms that the inhibition effectiveness of the PCCs is influenced by the phosphorus content in the PCC molecule rather than by the structure of the molecule. The burning velocity of a stoichiometric C_3H_8/air mixture and the extinction strain rate of a nonpremixed counterflow $CH_4/O_2/N_2$ flame doped with trimethylphosphate were calculated. Satisfactory agreement between experimental and modeling results confirms the conclusion that the reactions of phosphorus oxyacids with radicals are responsible for flame inhibition.

Keywords: Phosphorus-containing compounds; Inhibition; Suppression; Burning velocity; Extinction strain rate

---

1. Introduction

In the search for fire suppressants (FS) to replace halon 1301 (CF_3Br), a number of chemical compounds have been examined [1,2]. Among the most promising alternatives are phosphorus-containing compounds (PCCs). The synthesis of these compound is difficult, and thus they have not been thoroughly investigated. It has been shown previously [3–6] that the inhibition effect of PCCs is related to the catalysis of H and OH recombination by phosphorus oxides and oxyacids. In premixed flames, the catalytic cycle involving the reactions $H + PO_2 + M \rightarrow HOPO + M$ and $HOPO + OH \rightarrow H_2O + PO_2$ prevails. In a nonpremixed methane/air flame, there is a different set of key reactions responsible for inhibition: $H + PO_2 + M \rightarrow HOPO + M$ and $HOPO + H \rightarrow H_2 + PO_2$ [3]. In addition, it has been shown [6] that P-bearing oxyacids such as $HOPO_2$ play an important role in flame suppression. Although a considerable number of papers have been published in this area, there are still many problems to be solved.

The primary methods for evaluating the effectiveness of FS compounds consist of determining: (1) the extinguishing concentration of FS

---

[*] Corresponding author. Fax: +7 3832 342350.
E-mail address: korobein@ns.kinetics.nsc.ru (O.P. Korobeinichev).

1540-7489/$ - see front matter © 2004 The Combustion Institute. Published by Elsevier Inc. All rights reserved.
doi:10.1016/j.proci.2004.07.003

(cup-burner), (2) the dependence of extinction strain rate (ESR) on dopant loading in nonpremixed counterflow flames, and (3) the dependence of premixed flame speed on inhibitor loading. In fact, these techniques simulate various types of flames.

The goal of the present study was to improve our understanding of the inhibition mechanism by investigating the inhibition effectiveness of PCCs of various molecular structures in various types of flames (premixed and nonpremixed) and by comparing experimental and modeling data on the burning velocity of a premixed C_3H_8/air mixture and the extinction strain rate of a nonpremixed counterflow $CH_4/O_2/N_2$ flame doped with PCCs.

2. Experimental

2.1. Premixed burner

Burning velocity was measured using a Mache–Hebra nozzle burner [7] and the total area method [8] from flame images, as was done by Linteris and Truett [9]. The burner consisted of a 27-cm quartz tube with an area contraction ratio of 4.7 (over a 3-cm length) and a nozzle exit with an inner diameter of 1 cm. The nozzle contour was designed to obtain a straight-sided visible image of the flame cone. The burning velocity was measured using digitized images of visible cones obtained by CCD. The estimated confidence interval for burning velocity was about 5%. To evaluate the influence of heat losses from the flame to the burner on measured values, the speed of propane/air undoped flames of various stoichiometries was measured at $T_0 = 298$ K. The results were compared with experimental data obtained using alternative techniques [10,11]. In the equivalence ratio range (0.9–1.2) of combustible mixtures, there is good agreement between the literature and our data. For combustible mixtures having equivalence ratios of 1.3 and 0.8, the deviation is 15–20%. The comparison of the data obtained shows that the total area method from an image of a flame stabilized on a Mache–Hebra nozzle burner is suitable for measuring speeds of near-stoichiometric flames. To verify the measurement accuracy, an image of the flame was taken through a light filter. The filter isolated the emission of radiation by CH radicals at 431.4 nm. It was demonstrated that the total areas of the flame cone measured from visual images and using the filter differ by ± 2%. The combustible mixture included dry air and C_3H_8 containing about 4% C_4H_{10}. Gas flows were measured with a mass flow controller (MKS Instruments, model 1299S) calibrated with a wet gas meter with an accuracy of ± 1%. The volumetric flow rate of the combustible mixture was 3.3 slpm. The burner temperature was maintained at 95 °C. Table 1 lists the tested organophosphorus compounds and their boiling points. In addition, $POCl_3$ and a 60% water solution of H_3PO_4 were tested. PCCs were introduced into the gas flow using a nebulizer and a syringe pump. The inner diameter of the nebulizer nozzle was 0.1 mm, the walls of the central capillary were 0.04 mm thick, and the annular gap was 0.05 mm. The working pressure of the nebulizer was 5 atm. The mass-median diameter of the aerosol droplets of 30 and 80% solutions of glycerin in water varied from 10 to 20 μm, as determined by a five-stage cascade impactor [12]. The solution viscosity approximated the viscosity of trimethylphosphate (TMP) and $(HCF_2CF_2CH_2O)_3PO$. The nebulizer was installed in the lower part of the burner. The evaporation time for the aerosol drops was evaluated from the formula

$$\tau = \frac{\rho d_0^2}{8Dc},$$

where d_0 is the drop diameter, ρ is the density of a liquid PCC, D is the diffusion coefficient, and c is the saturated vapor concentration of the PCC. For evaluation of evaporation rate of OPC, the diffusion coefficient $D = 0.1\ \mathrm{cm^2/s}$ was taken. This value is typical for the species with molecular mass of about 140. Estimates show that at the given temperature, the evaporation time of PCC drops was much less than the residence time of the drops in the combustible mixture flow. Thus, when a PCC reached the flame, it was in the vapor state. The accuracy of PCC loading into the unburned gases was about ± 40 ppm. At 25 °C, the unburned gases reaching the flame contained both saturated PCC vapor and aerosol. To account for the deposition of PCCs inside the burner, the combustible mixture flow was passed through a

Table 1
PCCs investigated and their boiling points

No.	PCC	Boiling point (°C) at pressure (Torr)
1	$(CH_3O)_3PO$, TMP	180/760
2	$(C_2H_5O)_3PO$	215/760
3	$(CF_3CH_2O)_3PO$	187/760
4	$(HCF_2CF_2CH_2O)_3PO$	90/0,5
5	$(C_3F_7CH_2O)_3PO$	97/2,5
6	$(CH_3O)_2$ $P(O)CH_3$, DMMP	181/760
7	$(C_2H_5O)_2P(O)CH_3$	194/760
8	$(CF_3CH_2O)_2P(O)CH_3$	193/760
9	$(C_3F_7CH_2O)_2P(O)_3$	92/9
10	$(C_3F_7)_3PO$	144/760
11	$(CH_3O)_3P$	111/760
12	$(C_2H_5O)_2P(O)H$	204/760
13	$(CF_3CH_2O)_2P(O)H$	194/760
14	$(C_2H_5O)_3P$	158/760
15	$(CF_3CH_2O)_3P$	131/760
16	$(HCF_2CF_2CH_2O)_3P$	95/3
17	$(CF_3CH_2O)_2P(O)CF_3$	147/760
18	$(CF_3CH_2O)_2PO(OCH(CF_3)_2)$	83/10
19	$POCl_3$	105/760
20	H_3PO_4 60% water solution	—
21	$(HCF_2CF_2CH_2O)_2P(O)CH3$	115/6

filter that entrapped the PCC vapor and aerosol drops. This allowed us to determine the actual PCC concentration in the flame.

2.2. Counterflow burner

The effect of PCC fire suppressants on the ESR of an atmospheric nonpremixed counterflow CH_4/N_2–O_2/N_2 (0.2/0.8–0.4/0.6) flame was studied using a counterflow burner similar to that described by MacDonald et al. [13]. The inner diameter of the burner nozzles was 6.8 mm and the distance between the nozzles was 6.8 mm. The nitrogen flow was used as a sheath. The burner was aligned upright. The temperature of the oxidizer flow was kept at 100 °C to prevent PCCs condensation inside the burner. The oxidizer and fuel flow rates were set and controlled by mass flow controllers, which were operated by a computer. PCCs were added to the oxidizer using of a nebulizer and a syringe pump as described above. The ESR was measured by increasing the flow rates of the flame components until the flame was quenched. The procedure for evaluating the ESR was described earlier in [14]. The strain rate was calculated according to the equation [15]

$$a = \frac{2V_{\mathrm{ox}}}{L}\left(1 + \frac{V_{\mathrm{fuel}}}{V_{\mathrm{ox}}}\sqrt{\frac{\rho_{\mathrm{fuel}}}{\rho_{\mathrm{ox}}}}\right),$$

where V is the stream velocity, ρ is the stream density, and L is the separation distance between the nozzles. The typical value of the strain rate for flames varied from 100 to 800 s^{-1} and depended on the fuel/oxidizer ratio and the burner design. In our experiment without loading PCCs, the ESR was 750 s^{-1}.

2.3. Cup-burner technique

The effectiveness of PCC suppression of a nonpremixed flame was determined using the cup-burner technique. The cup burner used is a reduced variant of a standard cup burner [16,17] with some design changes. The fuel used was *n*-heptane. The cup burner was used as a chimney and consisted of a Pyrex tube with an inner diameter of 5.5 cm and a length of about 65 cm. The bottom of the tube was heated electrically to prevent condensation of PCC vapors. PCCs were introduced into the air flow using a nebulizer, which was described above. The volumetric flow rate of air through the nebulizer at the specified pressure was 1.0–0.95 slpm. Upon heating, the air with PCC drops flowed upward at a rate of 10 slpm moved. Although, PCCs usually evaporated, complete evaporation did not occur for low-volatility PCCs or for H_3PO_4. The cup has an upward conical expansion with a 30° angle. At the solution's top edge, the cup diameter was 13 mm. The air temperature near the cup was kept at 75 °C and the air velocity was ≈10 cm/s. Feeding of PCCs through the nebulizer was begun after flame ignition and establishment of a steady-state flame height of 4.5–5 cm, which took 2 min. The CO_2 flow was introduced in the air flow in discrete steps until the flame was extinguished. This method, described by Linteris [18], makes it possible to compare the suppression effectiveness of different FSs over a wide range of concentrations and to determine the extinguishing concentrations of FSs quite precisely. In studying flame suppression with volatile PCCs, we did not need to take into account deposition inside the chimney because the drops evaporated in the flow at a temperature of 75 °C. The mole fraction of the saturated vapor of TMP at this temperature is 0.014. But in the case of nonvolatile FSs such as a 60% water solution of orthophosphoric acid, part of the compound deposited inside the chimney and did not reach the flame. These losses were taken into account by measuring the concentration of the acid (in the form of an aerosol) near the cup. For this, a dye was added to the solution, and the aerosol was trapped by a filter. An analysis of the quantity of the aerosol deposited on a filter yielded the real concentration of H_3PO_4 in the experiment. An important parameter determining the drop size distribution is the ratio of the flow rates of air and liquid PCCs. It imposes restrictions on the upper level of PCC concentrations investigated in the present work.

3. Modeling

The burning velocity of a stoichiometric C_3H_8/air mixture was calculated as a function of TMP concentration using the PREMIX and CHEMKIN-II codes [19,20], the kinetic model for flame inhibition by TMP at atmospheric pressure proposed and updated by Korobeinichev et al. [21,22], and the mechanism for propane oxidation developed by Konnov [23]. The ESR of a nonpremixed counterflow $CH_4/O_2/N_2$ flame was modeled using the OPPDIF code from the CHEMKIN II Suite [24]. The GRI-MECH 3.0 mechanism for methane oxidation [25] and the same kinetic model for flame inhibition by TMP [22] were employed. In the calculations of the ESR of the counterflow flame mixture, averaged diffusion velocities and a potential flow boundary condition were used, and thermal diffusion was neglected.

4. Results and discussion

4.1. Effect of PCCs on burning velocity of stoichiometric C_3H_8/air mixture

The dependence of the burning velocity of a premixed stoichiometric C_3H_8/air mixture on PCC loading is given in Fig. 1. The data show that in loading up to 4500 ppm, the examined PCCs, including $POCl_3$ and water solutions of H_3PO_4, have similar inhibition effectiveness, which is higher than that of CF_3Br (per one molecule). Experimentally, we have not observed any noticeable increase of inhibition effectiveness of phosphorus compounds due to presence of fluorine in the molecules. For example, for pairs of compounds $(C_2H_5O)_3P$–$(CF_3CH_2O)_3P$, $(C_2H_5O)_2P(O)H$–$(CF_3CH_2O)_2P(O)H$ the data are exactly the same, and for $(C_2H_5O)_3PO$–$(CF_3CH_2O)_3PO$, the effectiveness of the fluorinated compound is 3% higher in the premixed flame. The calculated speed of the TMP-doped flame is presented in Fig. 1. The modeling and experimental results are in good agreement.

Sensitivity analysis [26] of the speed of a stoichiometric premixed C_3H_8/air flame was performed to specify the most important stages responsible for inhibition. To make a correct conclusion about importance of the stage, sensitivity coefficients of flame speed were evaluated by increasing and decreasing the rate constants of key reactions five times. The rate constants of the most important six reactions and sensitivity coefficients ξ are presented in Table 2. Here $\xi_{k/5} = [(u_k - u_{k/5})/u_k] \times 100$ and $\xi_{k \times 5} = [(u_k - u_{k \times 5})/u_k] \times 100\%$, where u_k is the burning velocity at a specified rate constant, $u_{k/5}$ and $u_{k \times 5}$ are the burning velocities at rate constants decreased and increased by a factor of 5, respectively. An increase of the pre-exponential factor A of reaction one (which is a stage of the catalytic cycle with participation of HOPO) from $A/5$ to $A \times 5$, results in a decrease of calculated burning velocity from 40 to 31 cm/s (burning velocity in the undoped mixture is 44.3 cm/s). The effect of the rate constant of the first reaction on the burning velocity is much higher than that of the other reactions.

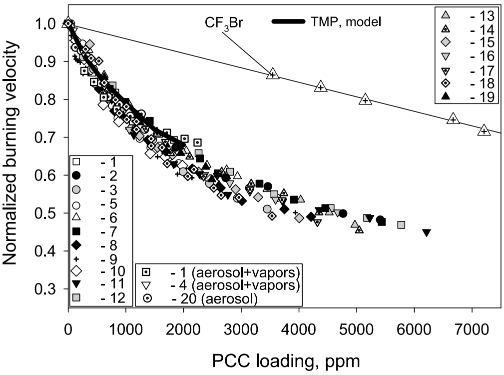

Fig. 1. Normalized burning velocity of stoichiometric premixed C_3H_8/air flame as a function of PCCs loading. Numbering of the compounds corresponds to that in Table 1.

Calculations of the burning velocity of the mixture doped with TMP and dimethyl methylphosphonate (DMMP) using the kinetic mechanisms for flame inhibition [4,27,28] also demonstrated good agreement with experimental results. The discrepancy between numerical and experimental data is less than 5%. These mechanisms differ from the mechanism of [21] in the initial stages of DMMP and TMP destruction. The rate constants of the key reactions (final conversions of oxyacids) in the mechanism of [21] differ slightly from those in [4,27,28]. For example, the pre-exponential factors of the most important reaction $H + PO_2 + M = HOPO + M$ varies by a factor of 1.5–2 in all above kinetic models. This supports the theory that the inhibition effectiveness is determined by the presence of phosphorus atoms in a PCC molecule but not by the structure of the molecule. The inhibition is caused by catalytic cycles of reactions of P-bearing species with H and OH radicals (for example, reactions 1 and 4 in Table 2), resulting in chain termination [3,27].

4.2. *Extinction strain rate of a nonpremixed counterflow CH_4/N_2–O_2/N_2 flame*

Normalized ESRs for a CH_4/N_2–O_2/N_2 flame versus OPC loading are presented in Fig. 2. The

Table 2
The rate constants [expressed as $k = A\,T^n \exp(-E/RT)$] of elementary reactions responsible for inhibition effect and ξ-coefficients of sensitivity for burning velocity (in %) of stoichiometric C_3H_8/air flame doped 1000 ppm of TMP

No.	Reaction	A[a]	n	E[a]	$\xi_{k/5} = (u_k - u_{k/5}/u_k) \times 100\%$[b]	$u_{k/5}$	$\xi_{k \times 5} = (u_k - u_{k \times 5}/u_k) \times 100\%$[b]	$u_{k \times 5}$
1	$H + PO_2 + M = HOPO + M$	9.73×10^{24}	−2.04	2696	−12.7	40	12.4	31.1
2	$O + HOPO = PO_2 + OH$	1.58×10^{13}	0.00	0	−4.6	37.1	7.5	32.73
3	$OH + PO_2 + M = HOPO_2 + M$	1.6×10^{24}	−2.28	1191	1.8	34.9	−5.1	37.3
4	$OH + HOPO = H_2O + PO_2$	3.16×10^{12}	0.00	0	−2.1	36.2	4.76	33.8
5	$H + HOPO_2 = H_2O + PO_2$	6.32×10^{12}	0.00	49867	−1.7	36.1	3.5	34.25
6	$O + HOPO_2 = O_2 + HOPO$	6.32×10^{12}	0.00	34426	0.3	35.39	0.34	35.36

[a] Units are mole, cm^3, s, J.

[b] u_k—burning velocity at recommended rate constant ($u_k = 35.5$ cm/s); $u_{k/5}$—burning velocity at rate constant reduced five times, $u_{k \times 5}$—burning velocity at rate constant increased five times. Units are cm/s.

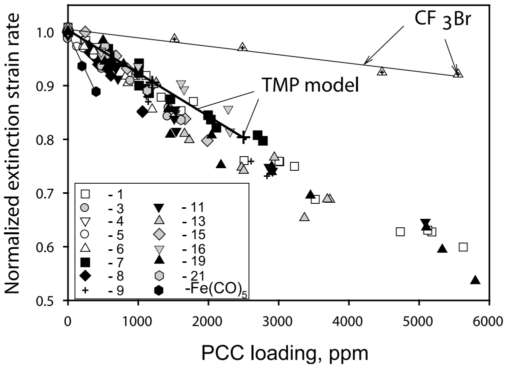

Fig. 2. Normalized extinction strain rate of the methane/O_2/N_2 flame as a function of PCCs and other suppression additives loading. Numbering of compounds corresponds to that in Table 1.

figure also gives our experimental results for CF_3Br and literature data for iron pentacarbonyl ($Fe(CO)_5$) obtained by Reinelt and Linteris [29] using a burner of different design and different composition of gas flows. The fire suppression effectiveness in terms of ESR was defined as the fractional reduction in global ESR divided by the mole fraction of phosphorus χ_P in the flame [3]:

$$\mathrm{Effectiveness}_q = \frac{a_{q,0} - a_q}{a_{q,0}} \frac{1}{\chi_P}.$$

The subscript q indicates that the strain rate measurement was made under extinction conditions, and the subscript 0 denotes the value for the undoped flame. All tested PCCs show similar fire suppression effectiveness (within a confidence interval of ± 5%) in loading up to 1000 ppm. For this flame with dopant loading below 1000 ppm, all tested compounds are approximately seven times more effective than halon 1301 and about three times less effective than $Fe(CO)_5$ [29]. This result supports the suggestion that the fire suppression effectiveness is determined by the concentration of phosphorus oxides and oxyacids, which in turn depends weakly on the structure of PCCs molecule.

The normalized ESR for TMP-doped (1200 and 2500 ppm) flames was calculated and compared with experimental results, as was done by Wainner et al. [27]. Similar results were reported by Wainner et al. [27] and Jayaweera [30]. As can be seen from Fig. 2, the modeling results are in good agreement with experimental data. Thus, the experiment shows that the ESR decreases by 10 and 20% for dopant concentrations of 1200 and 2500 ppm, respectively, whereas numerical calculations predict a decrease of 9.4 and 18.8% for the same TMP concentrations.

To specify the most important reactions for suppression of diffusive counterflow flame, the sensitivity coefficients of ESR change with respect to variation of rate constants of six reactions were evaluated using the procedure similar to sensitivity analysis for the premixed flame. The preexponential factors of the rate constants were in turn increased and decreased in four times, and ESRs were estimated for initial, increased, and decreased rate constants. The sensitivity coefficients were defined as

$$\zeta_{k/4} = \frac{ESR_k - ESR_{k/4}}{ESR_k} \times 100 \text{ and}$$

$$\zeta_{k\times 4} = \frac{ESR_k - ESR_{k\times 4}}{ESR_k} \times 100\%,$$

where $ESR_{k/4}$ and $ESR_{k\times 4}$ correspond to the preexponential factors of the rate constants decreased and increased by a factor of 4, respectively, ESR_k corresponds to the initial value of the rate constants. The sensitivity coefficients ζ and ESRs calculated are given in Table 3. The data presented in Table 3 demonstrate that the decrease in rate constants of all reactions results in a fourfold increase in ESR, in other words, in a reduction of the flame suppression effectiveness. The effect of the change in the rate constant of reaction 1 is the most significant. However, the fourfold increase all of the rate constants showed that increasing the rate constant of only reaction 1 results in a rise of suppression efficiency. The increase in the rate constants of other reactions reduces the flame suppression effectiveness. This agrees with the results on the influence of this reaction on the speed of the premixed flame (Table 2). ESR change is apparently most sensitive to increasing the rate constant of reaction 3. However, the increase in the rate constant of reaction 3 in four cases resulted not an increase but a decrease in suppression efficiency. Here, the ESR value at the increased rate constant exceeded the ESR value in an undoped flame. Thus, the reasonable value of a rate constant of reaction 3 should not considerably exceed its value represented in Table 2. Apparently, the ESR is more of a function of rate constants of the above reactions than the speed of a premixed flame.

4.3. Suppression of a nonpremixed coflow n-heptane flame

The results of investigation of the FS effectiveness in cup-burner tests are presented in Fig. 3 as curves of the CO_2 extinguishing concentration versus PCC loading. The symbols in the diagram correspond to the suppression conditions of a diffusion *n*-heptane flame; thus, the flame can exist only at lower concentrations of CO_2 and/or PCCs. Figure 3 also shows data for CF_3Br. It is evident that in the range of concentrations from 0 to 5000 ppm, a large number of PCCs, including aqueous H_3PO_4 aerosol and $POCl_3$ vapor, have similar flame suppression effectiveness. All

Table 3
The elementary reactions responsible for inhibition effect and ζ-coefficients of sensitivity for extinction strain rate of counterflow $CH_4/O_2/N_2$ flame doped with 1200 ppm TMP

No.	Reaction	$\zeta_{k/4} = [(ESR_k - ESR_{k/4})/ESR_k] \times 100\%$	$ESR_{k/4}$[a]	$\zeta_{k \times 4} = [(ESR_k - ESR_{k \times 4})/ESR_k] \times 100\%$	$ESR_{k \times 4}$[a]
1	$H + PO_2 + M = HOPO + M$	−7.8	1151.6	5.22	1012
2	$O + HOPO = PO_2 + OH$	−6.39	1136.1	−0.58	1074
3	$OH + PO_2 + M = HOPO_2 + M$	−0.58	1074	−7.27	1145.4
4	$OH + HOPO = H_2O + PO_2$	−4.36	1114.4	−1.45	1083.3
5	$H + HOPO_2 = H_2O + PO_2$	−4.06	1111.2	−0.58	1074
6	$O + HOPO_2 = O_2 + HOPO$	−5.23	1123.7	−1.74	1086.4

ESR_k—extinction strain rate at recommended rate constant, $ESR_{k/4}$ and $ESR_{k \times 4}$—extinction strain rates at rate constant reduced and increased in four times, respectively, $ESR_k = 1068\ s^{-1}$. Extinction strain rate calculated for undoped flame was $1117\ s^{-1}$.

[a] Units are s^{-1}.

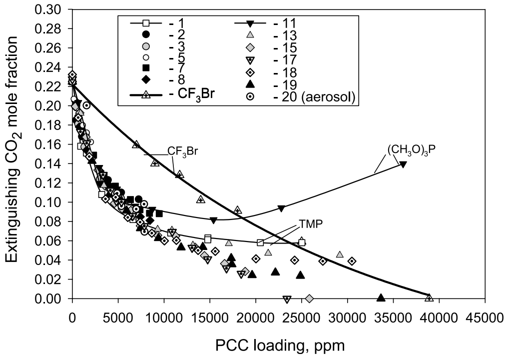

Fig. 3. The dependencies of CO_2 extinguishing concentrations on PCCs loading for the cup-burner *n*-heptane flame. Numbering of compounds corresponds to that in Table 1.

of these compounds, in both premixed and diffusion flames, are more effective than CF_3Br. For loading of 10,000 ppm (1% by volume) and higher, a decrease or no further growth in the fire suppression effectiveness was observed for several compounds (Fig. 3). The extinguishing concentration of CO_2 increased with the increase in the PCC concentration. A particularly strong decrease in the effectiveness was found for trimethylphosphite [$(CH_3O)_3P$]. Such unusual behavior can be explained by a competition of two processes. The first process is flame suppression, which is enhanced with PCC loading. The second is related to an increase in heat release and an increase in the final combustion temperature due to combustion of PCC vapors. At high $(CH_3O)_3P$ concentrations, heat release from PCC combustion dominates over fire suppression. This is supported by observation of a secondary flame in the upper part of the chimney for a number of PCCs. However, at low PCC loading (below 5000 ppm), the first process prevails over the second one. A reduction in the suppression effectiveness with an increase in PCC loading was not observed in premixed (Mache–Hebra nozzle burner) and counterflow flames because the experiments were carried out for appreciably lower loadings of PCCs. The inhibition and suppression effectivenesses for flames of different types were compared using the formula

$$\Phi = (\Delta X/X_0)(1/\chi_p),$$

where $\Delta X/X_0$ is the relative change of a particular parameter (burning rate, ESR, or extinguishing concentrations) and χ_p is the corresponding mole fraction of a compound.

A comparison of the inhibition effectiveness of PCCs in premixed and nonpremixed flames (cup-burner and opposed-jet burner techniques) shows (Table 4) that for loading up to 5000 ppm, all PCCs have similar effectiveness, which is higher than that of CF_3Br. Even for nonflammable PCCs, which do not exhibit a typical regularity, the effectiveness at loading about 20,000 ppm varies appreciably, not due to experimental errors, but because their extinguishing concentrations range 2.3–3.4% by volume. Thus, the data obtained indicate that the suppression effect of PCCs, including an aqueous solution of H_3PO_4, is due primarily to the presence of the phosphorus atom in the PCC molecules.

Table 4
Comparison of effectiveness of PCCs relative to CF_3Br as a ratio of Φ_{PCC} to Φ_{CF_3Br} obtained using three different techniques; $\Phi = (\Delta X/X_0)(1/\chi_p)$

C, ppm	Effectiveness of PCCs relative to CF_3Br		
	Mache–Hebra burner	Counterflow burner	Cup-burner
1000	5.8	5.0	5.5
2000	4.5	5.6	3.8
4000	3.1	5.4	2.9
10,000	—	—	1.8[a]
20,000	—	—	1.3[a]

[a] Averaged effectiveness for $(CF_3CH_2O)_3P$, $(CF_3CH_2O)_2P(O)CF_3$, and $POCl_3$.

5. Conclusions

A study was performed of the influence of some PCCs (fluorinated and nonfluorinated phosphates, phosphonates, and phosphites) on the speed of a stoichiometric premixed C_3H_8/air flame, the extinction strain rate of a nonpremixed counterflow $CH_4/N_2–O_2/N_2$ flame, and the extinction of a coflow nonpremixed *n*-heptane/air flame.

All PCCs had similar dependencies of burning velocities, extinction strain rates, and extinction volume fractions of CO_2 on PCC loading in the range of mole fractions 0–7000 ppm. This confirms that the inhibition effectiveness of the PCCs is affected by the phosphorus content in the PCC molecule rather than by the structure of the molecule. The inhibition mechanism was validated by comparing experimental and modeling data for the burning velocity of a stoichiometric C_3H_8/air mixture and for the extinction strain rate of an counterflow $CH_4/N_2–O_2/N_2$ flame.

Acknowledgments

This work was supported by the US Civilian Research and Development Foundation under Grant No. RC1-2386-NO-02 and partly by Grant No. 37 of Rus. Ac. Sci. SB. The authors thank T. Jayaweera for help in modeling of counterflow flame, and E.E. Nifantev, I.Y. Kudryavtsev, and E.I. Goryunov for preparing organophosphorus compounds for our tests.

References

[1] R.E. Tapscott, R.S. Sheinson, V.I. Babushok, M.R. Nyden, R.G. Gann, *Alternative Fire Suppressant Chemicals: A Research Review with Recommendations*, NIST Technical Note 1443, 2001.

[2] R.G. Gann, *FY2001 Annual Report Next Generation Fire Suppression Technology Program (NGP)*, NIST Technical Note 1445, 2002.

[3] M.A. MacDonald, F.C. Gouldin, E.M. Fisher, *Combust. Flame* 124 (4) (2001) 668–683.

[4] P.A. Glaude, H.J. Curran, W.J. Pitz, C.K. Westbrook, *Proc. Combust. Inst.* 28 (2001) 1749–1756.

[5] V.I. Babushok, W. Tsang, *Combust. Flame* 123 (4) (2000) 488–506.

[6] O.P. Korobeinichev, T.A. Bolshova, V.M. Shvartsberg, A.A. Chernov, *Combust. Flame* 125 (1–2) (2001) 744–751.

[7] H. Mache, A. Hebra, *Sitzungsber. Osterreich. Akad. Wiss. Abt. IIa* 150 (1941) 157.

[8] G.E. Andrews, D. Bradley, *Combust. Flame* 18 (1972) 133–153.

[9] G.T. Linteris, G.T. Truett, *Combust. Flame* 105 (1–2) (1996) 15–27.

[10] A. Van Maaren, L.P.H. de Goey, *Combust. Sci. Technol.* 102 (1994) 309–314.

[11] C.M. Vagelopoulos, F.N. Egolfopoulos, C.K. Law, *Proc. Combust. Inst.* 25 (1994) 1341–1347.

[12] V.A. Marple et al., in: K. Willeke, P.A. Baron (Eds.), *Aerosol Measurement: Principles, Techniques, and Applications.* Van Nostrand Reinhold, New York, 1993, p. 212.

[13] M.A. MacDonald, T.M. Jayaweera, E.M. Fisher, F.C. Gouldin, *Proc. Combust. Inst.* 27 (1998) 2749–2756.

[14] M.A. MacDonald, T.M. Jayaweera, E.M. Fisher, F.C. Gouldin, *Combust. Flame* 116 (1999) 166–176.

[15] K. Seshadri, F.A. Williams, *Int. J. Heat Mass Transfer* 21 (1978) 251–253.

[16] R. Hirst, K. Booth, *Fire Technology* 13 (1977) 296.

[17] ISO, *Gaseous Fire Extinguishing Systems—Physical Properties and System Design*, Draft International Standard, ISO/DIS 14520–1, 1998.

[18] G.T. Linteris, *Halon Options Technical Working Conference (HOTWC)*. Center for Global Environmental Technologies, Albuquerque, NM, 2001, pp. 187–197.

[19] R.J. Kee, J.F. Grcar, M.D. Smooke, J.A. Miller, *PREMIX*, Report No. SAND85-8240, Sandia National Laboratories, 1985.

[20] R.J. Kee, F.M. Rupley, J.A. Miller, *CHEMKIN-II: A Fortran Chemical Kinetics Package for the Analysis of Gas Phase Chemical Kinetics*, Report No. SAND89-8009B, Sandia National Laboratories, 1989.

[21] O.P. Korobeinichev, S.B. Ilyin, T.A. Bolshova, V.M. Shvartsberg, A.A. Chernov, *Combust. Flame* 121 (2000) 593–609.

[22] O.P. Korobeinichev, A.L. Mamaev, V.V. Sokolov, T.A. Bolshova, V.M. Shvartsberg, *Halon Option Technical Working Conference (HOTWC)*. Center for Global Environmental Technologies, Albuquerque, NM, 2001, pp. 173–186.

[23] A.A. Konnov, *Detailed Reaction Mechanism for Small Hydrocarbons Combustion*. 2000 Release 0.5. Available from: <http://homepages.vub.ac.be/~akonnov/>.

[24] A.E. Lutz, R.J. Kee, J.F. Grcar, F.M. Rupley, *Chemkin Collection, Unlimited Release*, Sandia National Laboratories, Livermore, CA, 1997.

[25] G.P. Smith, D.M. Golden, M. Frenklach, N.W. Moriarty, B. Eiteneer, M. Goldenberg, C.T. Bowman, R.K. Hanson, S. Song, W.C. Jr. Gardiner, V.V. Lissianski, Z. Qin, *GRI Mech 3.0*, 1999. Available from: <http://www.me.berkeley.edu/gri_mech/>.

[26] J. Warnatz, U. Maas, R.W. Dibble, *Combustion.* Springer-Verlag, Berlin, 1996, p. 89.

[27] R.T. Wainner, K.L. McNessby, R.G. Daniel, A.W. Miziolek, V.I. Babushok, *Halon Option Technical Working Conference (HOTWC)*, Center for Global Environmental Technologies, Albuquerque, 2000, pp. 141–153.

[28] V.I. Babushok, W. Tsang, *Third International Conference on Fire Research and Engineering*, Society of Fire Protection Engineers, Bethesda, 1999, p. 257.

[29] D. Reinelt, G.T. Linteris, *Proc. Combust. Inst.* 26 (1996) 1421–1428.

[30] Jayaweera, T.M., *Flame Suppression by Aqueous Solutions*, Ph.D. thesis, Cornell University, Ithaca, NY, 2002.

Comments

Greg Linteris, NIST, USA. For inhibition of flames by metallic compounds, we have found that loss of effectiveness is caused by condensation of active species to particles. I am wondering if this mechanism can be responsible for the loss of effectiveness of some of your OPCs. Did you see any evidence of particle formation (black sooty emission, surface coating, etc.) in the product stream behind your flames with OPCs at high loading?

Reply. It is noteworthy that a reduction of inhibition effectiveness of cup-burner flames at high loadings of OPC seems to be controlled by a number of factors. We do observe black sooty emission, surface coating, etc., in the product stream behind our flames with OPCs at high loading. So we agree that condensation of active species on soot particles can be one of these factors. At high OPC loading the flame becomes rich. A reduction of the inhibition effectiveness in rich premixed OPC-doped flames, which we observed experimentally and in modeling at $\phi > 1.2$, can be another factor. Finally, an additional heat release due to combustion of OPC can be the third factor.

•

John C. Mackie, University of Sydney, Australia. Some of your organophosphorus agents actually appear to show promotion at high additive levels. Did you carry out modeling at these levels to attempt to ascertain the reason for this effect?

Reply. We did not carry out modeling of flames stabilized on a cup burner, as we do not have a corresponding computer code. We also did not simulate premixed flames at high levels of OPC loading but we plan to do this. The experiments revealed that at a loading of 0.5–1%, such flames do not exist, but combustion does seem to proceed at a loading of 3–4%.